Supporting Information Appendix

Materials and Methods-

Synthesis of Gold Nanoprisms

Gold nanoprisms were synthesized according to literature methods reported by Millstone et al. (1-2) with minor differences. Briefly, gold nanoparticle seeds were first prepared by adding 1 mL of 0.01 M sodium citrate, 1 mL of 0.01 M $HAuCl_4$, and 1 mL of 0.10 M $NaBH_4$ consecutively to 36 mL of Nanopure water in a round bottom flask. The solution was stirred vigorously for 1 minute, then allowed to age for 2-4 hours. The resulting gold seeds are approximately 5 nm in diameter and 65 nM in concentration. Next a "growth solution" was prepared consisting of 9 mL of an aqueous solution of 0.05 M CTAB containing 50 μM NaI, 250 μL of 0.01M $HAuCl_4$, 50 μL of 0.10 M NaOH, and 50 μL of 0.10 M L-ascorbic acid. Addition of the aged gold seeds to the growth solution resulted in a purple solution containing gold nanoprisms and gold nanospheres over the course of 30 minutes. By varying the final seed concentration in the growth solution from 577 pM to 26 pM, nanoprisms with edge lengths ranging from 40 – 210 nm were synthesized. The thickness remained constant at 7.5 nm.

Small Angle X-ray Scattering Studies

SAXS measurements were made using the instrument at undulator beamline 12ID-C (17 keV) of the Advanced Photon Source at Argonne National Laboratory in Lemont, IL. The sample-to-detector distance was such as to provide a detecting range for scattering vector $q = 4\pi(\sin\theta)/\lambda$,where θ is the angle between the incident radiation and the scattering planes and λ is the radiation wavelength, of $0.01 < q < 0.20$ $Å^{-1}$. The scattering vector was calibrated using a silver behenate standard. Samples were placed in 1.5 mm quartz capillaries and irradiated for an exposure time of 0.1 sec. Scattered radiation was detected with a CCD area detector and radially averaged to produce 1-D plots of scattered intensity I(q) versus scattering vector q. All data were corrected for background scattering. Temperature control of samples was achieved using a custom-built Peltier device.

It is important to note that the nanoprism samples were super-saturated with CTAB and CTAB will start to crystallize out of the time scale of several hours. Great care was taken to ensure that all samples analyzed with SAXS did not have any visible CTAB crystals. If CTAB crystals were observed, the samples were dipped in luke-warm water and allowed to cool to room temperature before analysis with SAXS.

The nanoprism crystallites were determined to contain a total of 10 – 15 prisms. There are several possible reasons for the relatively small number of prisms per superlattice. In terms of energetics, the ratio of the total repulsive energy/attractive energy is not a function of the number of nanoprisms in the lattice and thus there may not be a strong preference for a new prism to attach to one column over another. If there is any preference, it is to increase the stability of the columnar superlattices, for example, by decreasing its surface energy. Additionally, it is possible that once the superlattices contain greater than ~15 prisms, they undergo a gravitational sedimentation process that selectively isolates them from the crystallization process.

Calculation of 1-D Electron Density Profile

To calculate the 1-D electron density profile ρ(z) of the nanoprism superlattices, it was necessary to extract the diffraction pattern solely from the lamellar stacks of prisms from the total I(q). To achieve this, scattering from the spherical gold nanoparticles and the CTAB micelles (assumed to be spherical) were fitted with two polydisperse sphere models (gold spheres and CTAB micelles) and were subtracted out of I(q) (Fig. S3A). Then, the integrated area of each of the 4 resolvable diffraction peaks was calculated and corrected for the Lorentz factor by multiplying the square of the peak positions by the integrated areas. At this point, if the amplitude and phase of each diffraction peak is known, the electron density profile can be simply obtained using a Fourier synthesis. The former is the square root of the corrected intensity. However, the phases are not known in this work. Fortunately, the presence of a center of symmetry along the direction perpendicular to the lamellar crystals simplifies the phase problem in this case: the phase of each diffraction peak can be assigned either +1 or -1 (3).

Since there are four resolvable diffraction peaks in our SAXS patterns, there can be a total of 16 combinations of phases (2*2*2*2). This number, however, can be reduced in half because of inversion symmetry since a set of phases (1,1,1,1) results in an identical electron density profile that will be obtained with (-1,-1,-1,-1). The electron density maps resulting from the 8 combinations are shown in Fig. S3B. It must be noted that the units of the electron density in these maps are arbitrary since the SAXS data were not measured on an absolute scale. As a starting point, the 7.5 nm thick gold nanoprisms should appear in ρ(z) as narrow regions of high electron density. Given our system, there should not be any other components that have an electron density that matches that of the gold nanoprisms. Additionally, the *d*-spacing of the lamellar superlattices is known from the SAXS data and thus two nanoprisms cannot be right next to each other in ρ(z). This means that half of the profiles are physically unreasonable (profiles 3, 5, 6, and 8). Of the remaining 4 profiles, 1 and 7 are identical, albeit shifted, and 2 and 4 are inverted. Between 1 (or 7) and 2 (or 4), profile 1, with regions of high electron density surrounded on either side by regions of low electron density, is chosen as the most probable one. The regions of high electron density, separated by approximately 30 nm, and low electron density on either side were assigned to the gold nanoprisms and the CTAB bilayer, respectively.

Anomalous Small Angle X-ray Scattering (ASAXS)

Anomalous X-ray scattering is a technique used to determine the location of an element of interest within a sample. The energy of the incident X-ray beam is tuned around an absorption edge of the element of interest and an electron density map as a function of energy can be calculated. In this work, the elements of interest are Au, since the nanoprisms that make up the lamellar superlattices and the spherical particles in the solution surrounding the superlattices are gold, and Br, since Br^- is the negative counterion of CTAB and the CTAB micelles are only ~25% dissociated (meaning the location of Br^- in the sample is a good indication of the location of the CTAB micelles). We did not attempt to calculate the electron density map of the lamellar nanoprism superlattices as a function of energy because the contribution of Br to the scattering pattern was predicted to be weak. Additionally, there was the concern of sample damage from repeated X-ray exposure since reliable quantitative ASAXS measurements require long exposure times. However, by plotting measured contrasts as a function of energy, it is possible to roughly determine the Au and Br distribution in the sample.

ASAXS studies were conducted around the Au L3 edge (11.919 keV) and the Br K edge (13.474 keV). To determine whether the CTAB micelles were located within the nanoprism superlattices, the scattering intensity for the gold nanoprism superlattices and the gold nanoparticle spheres in solution were compared. When the energy of the incident beam was tuned around 11.919 keV, there was not a significant difference between the integrated intensity of the first order diffraction peak (q_0) from the nanoprism superlattices, $I(q = q_0)_{prism}$, and the scattering intensity from the gold spheres, $I(q = 0)_{sphere}$ (Fig. S4A). This means that there is gold both within the lamellar superlattices (the nanoprisms) and in the surrounding solution (the spherical nanoparticles). At the Br edge, $I(q = q_0)_{prism}$ shows a sharp variation near the edge and remains nearly constant away from the Br edge (Fig. S4B). On the other hand, $I(q = 0)_{sphere}$ varies continuously and drops significantly below the edge. If the Br^- ions were homogeneously distributed within the nanoprism superlattices, meaning their concentration within the superlattices is equal to the average value in the surrounding solution, the two curves should nicely overlap as they do in Fig. S4A. If the concentration of Br^- ions within the nanoprism superlattices is greater than the average value of the surrounding solution, $I(q = q_0)_{prism}$ would show a more significant drop in intensity away from the absorption edge. The fact that $I(q = 0)_{sphere}$ drops more suggests that on average, there is more Br^-, and therefore more CTAB micelles, in the solution surrounding the nanoprism superlattices than in the solution between the superlattices. Additionally, sharper variation in $I(q = q_0)_{prism}$ around the Br edge may suggest that the Br located within the nanoprism superlattices is more localized (for example, closer to the nanoprism surface). However, the variation of intensity was not significant enough to conclusively determine the electron density map as a function of energy.

Small Angle Neutron Scattering (SANS)

SANS measurements were performed at the High Flux Isotope Reactor at Oak Ridge National Laboratory in Oakridge, TN. SANS data were collected to determine the average size of the CTAB micelles at different CTAB concentrations (0.05 M and 0.20 M) and temperatures (30˚C and 50˚C). The Percus-Yevick model for hard spheres (4) was used to calculate the average diameter of the CTAB micelles (d_{CTAB}). The micelles were assumed to be spherical for simplicity. The exclusion radius (R_e), defined as the distance from the center of each micelle to the point at which other micelles do not penetrate, was also calculated. The calculated values of d_{CTAB} and R_e are summarized in Table S1. In our SANS measurements, conducted on samples of as-synthesized samples of 145 nm edge length nanoprisms (with Au spheres and CTAB micelles), d_{CTAB} (nm) increased with increasing CTAB concentration and decreased with increasing temperature. This is consistent with studies of solutions of pure CTAB in the literature (5).

Including van der Waals Interactions in the Energy Minimization Calculations

To explore whether van der Waals forces play a significant role in the formation of the lamellar nanoprism superlattices, these interactions were added to our theoretical model. The van der Waals interaction energy is given by

$$E_{vdW} = -\frac{HA}{12\pi}\left[\frac{1}{\left(d - t_{prism}\right)^2} - \frac{2}{d^2} + \frac{1}{\left(d + t_{prism}\right)^2}\right]$$

where H is the Hamaker constant for gold across water (~10^{-19} J) (6-7).

Parameters for Theoretical Calculations of *d*-spacings

The parameters used in the theoretical calculations of the *d*-spacings of the nanoprism superlattices at various CTAB concentrations, temperatures, and ionic strengths are listed below.

CTAB Concentration (Fig.4B)

CTAB conc (M)	**Debye Length (nm)**	**N_{agg}**	**d_{CTAB} (nm)**	**Effective Charge**	**δ_{CTAB}**
0.05	2.69	139	5.38	0.26	0
0.075	2.27	149	5.58	0.24	0
0.10	2.03	160	5.80	0.23	0
0.15	1.78	180	6.24	0.20	0.59
0.20	1.68	201	6.68	0.17	0.85
0.25	1.67	221	7.12	0.14	0.78
0.30	1.74	242	7.56	0.10	0.68

Temperature (Fig. 5)

Temp (˚C)	**Debye Length (nm)**	**N_{agg}**	**d_{CTAB} (nm)**	**Effective Charge**	**δ_{CTAB}**
30	2.85	144	6.06	0.23	0
45	2.71	122	5.66	0.26	0
60	2.58	100	5.28	0.28	0

Ionic Strength (Fig. 6A)

NaCl conc (M)	**Debye Length (nm)**	**N_{agg}**	**d_{CTAB} (nm)**	**Effective Charge**	**δ_{CTAB}**
0	2.69	139	5.38	0.26	0
0.0025	2.47	139	5.38	0.26	0
0.0050	2.29	139	5.38	0.26	0
0.0075	2.14	139	5.38	0.26	0
0.0250	1.58	139	5.38	0.26	0
0.0500	1.22	139	5.38	0.26	0
0.0750	1.04	139	5.38	0.26	0
0.100	0.91	139	5.38	0.26	0

References

1. Millstone JE*, et al.* (2005) Observation of a Quadrupole Plasmon Mode for a Colloidal Solution of Gold Nanoprisms. *J Am Chem Soc* 127:5312-5313.
2. Millstone Jill E, Wei W, Jones Matthew R, Yoo H, & Mirkin Chad A (2008) Iodide ions control seed-mediated growth of anisotropic gold nanoparticles. *Nano Lett* 8:2526-2529.
3. Roe RJ (2000) *Methods of X-Ray and Neutron Scattering in Polymer Science* (Oxford University Press, New York), pp 155-209.
4. Muratov A, Moussaid A, Narayanan T, & Kats EI (2009) A Percus-Yevick description of the microstructure of short-range interacting metastable colloidal suspensions. *J Chem Phys* 131:054902.
5. Aswal VK & Goyal PS (2003) Selective counterion condensation in ionic micellar solutions. *Physical Review E* 67:051401.
6. Parsegian VA (2006) *Van der Waals Forces. A Handbook for Biologists, Chemists, Engineers and Physicists* (Cambridge University Press), pp 61-74.
7. Walker DA, Browne KP, Kowalczyk B, & Grzybowski BA (2010) Self-Assembly of Nanotriangle Superlattices Facilitated by Repulsive Electrostatic Interactions. *Angew Chem, Int Ed* 49:6760-6763.

Small Angle Neutron Scattering Data Characterizing CTAB Micelles

	0.05 M CTAB	**0.20 M CTAB**
30˚C	d_{CTAB} = 5.80 nm	d_{CTAB} = 6.02 nm
	R_e = 7.55 nm	R_e = 5.60 nm
50˚C	d_{CTAB} = 5.12 nm	d_{CTAB} = 5.14 nm
	R_e = 6.63nm	R_e = 4.87 nm

Table S1. Summary of SANS data used to characterize the CTAB micelles. The radius of the micelles (d_{CTAB}) and exclusion radius (R_e) were determined for CTAB concentrations of 0.05 M and 0.20 M at temperatures of 30˚C and 50˚C. R_e is defined as the distance from the center of each micelle to the point at which other micelles do not penetrate. Thus $2*R_e$ is a measure of the distance between 2 micelles (center to center) in solution.

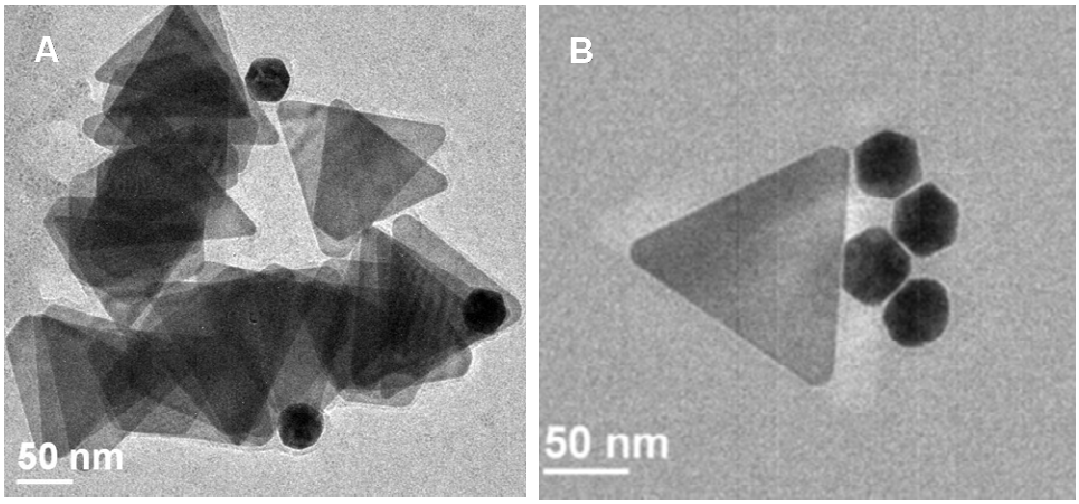

Fig S1. (A,B) Transmission Electron Microscope images of the 145 nm edge length gold nanoprisms and 38 nm gold nanoparticles formed in a typical synthesis.

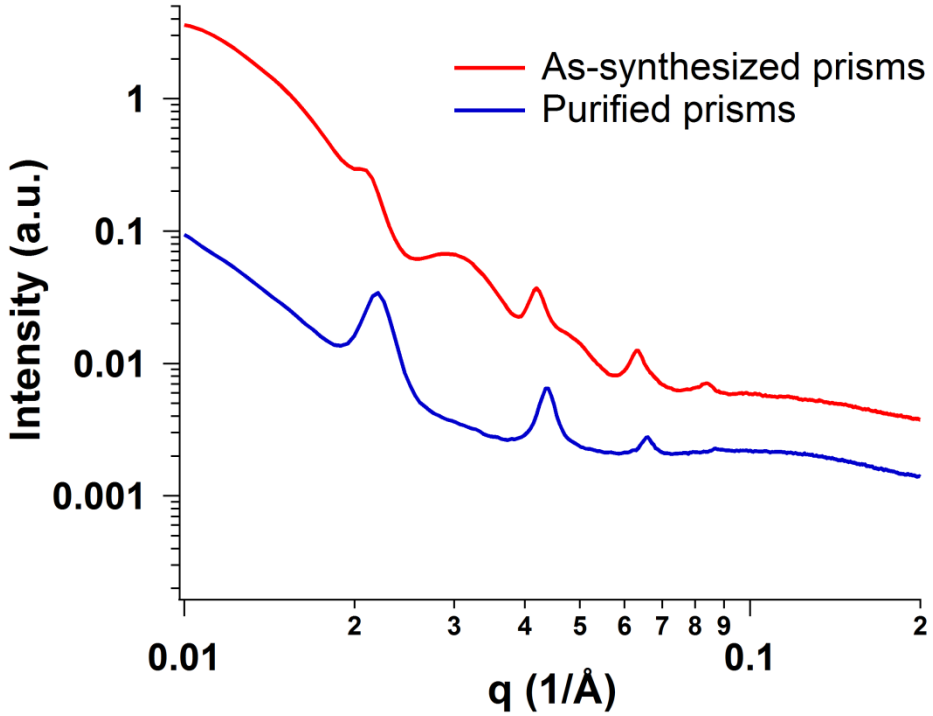

Fig. S2. One-dimensional SAXS profiles of the as-synthesized Au nanoprisms (145 nm edge length) and purified Au nanoprisms (145 nm edge length). Since the sample of as-synthesized prisms also contains spherical nanoparticles, the scattering pattern contains a background indicative of the form factor of spherical particles. The sample of purified prisms does not contain such a background. Most importantly, the sharp diffraction peaks for both samples are located at similar q values, indicating that the formation of the lamellar nanoprism superlattices is not affected by the presence of the spherical gold nanoparticles.

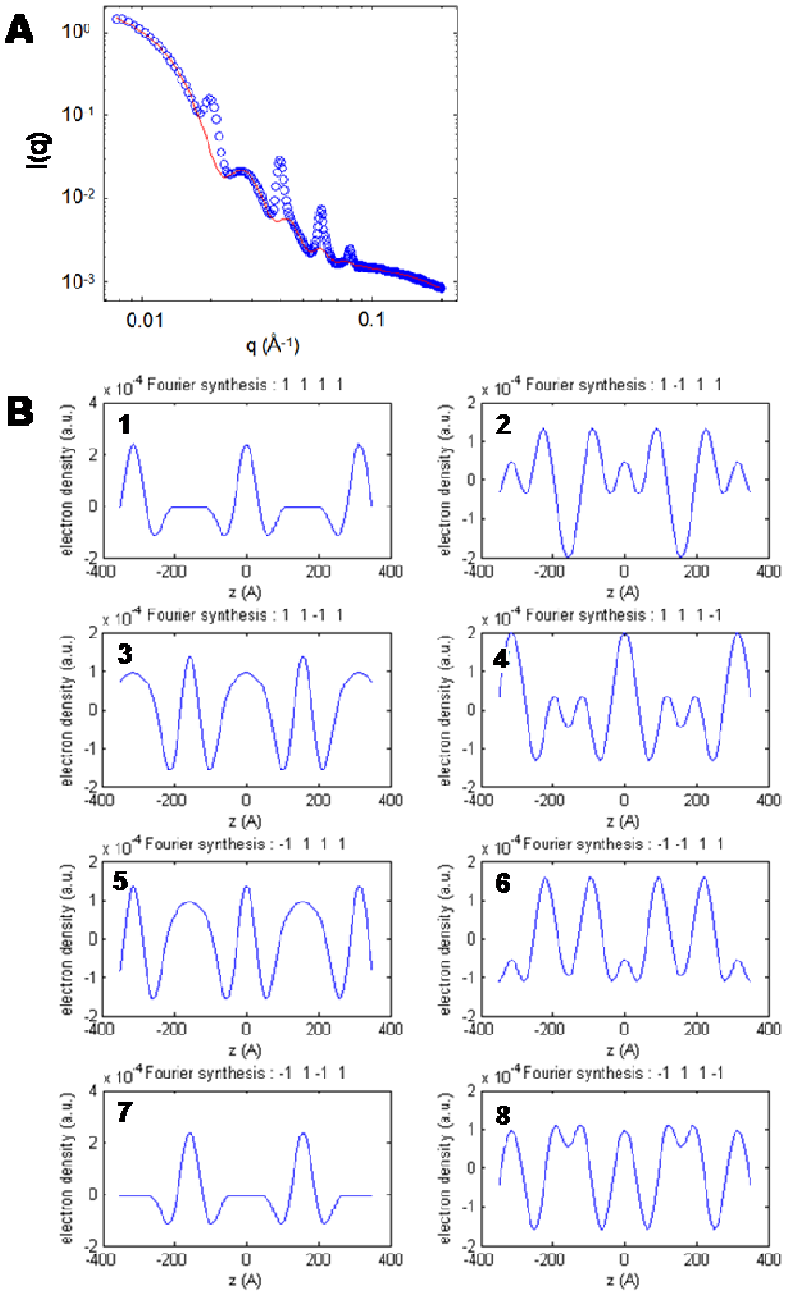

Fig. S3. Calculation of 1-dimensional electron density profile ρ(z) of the lamellar superlattices. (A) Measured SAXS data (blue circles) for a typical sample of as-synthesized nanoprisms containing 145 nm edge length gold nanoprisms, 38 nm diameter gold nanoparticles, and 6 nm diameter CTAB micelles, along with a fit (red solid line) of a model with two polydisperse spheres to allow for the extraction of the diffraction pattern solely from the nanoprism superlattices. (B) The 8 possible electron density maps derived from assigning a +1 or a -1 to each of the 4 diffraction peaks caused by the lamellar superlattices. Profiles 1 and 7, which are the same albeit shifted, were chosen as the most probable electron density profile for the lamellar superlattices.

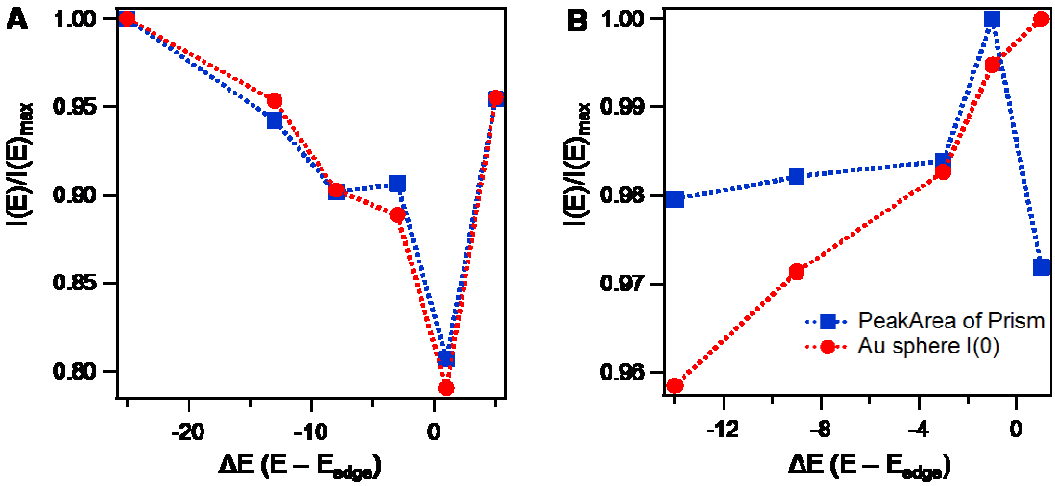

Fig. S4. Anomalous small angle X-ray scattering intensities for the gold nanoprism superlattices (blue squares) and the gold nanoparticle spheres in solution (red circles) when the incident X-ray beam was tuned around (A) the Au L3 edge (11.919 keV) and (B) the Br K edge (13.474 keV). I(0) intensities from the gold nanoparticle spheres and the areas of the diffraction peaks from the nanoprism superlattices were normalized by the maximum intensities of each energy scan.

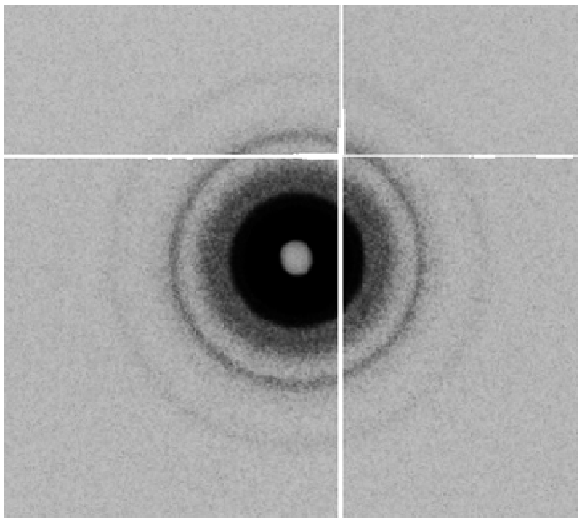

Fig. S5. Two-dimensional SAXS pattern of the as-synthesized Au nanprisms (145 nm edge length) in solution. The presence of rings indicates random orientation of the superlattices relative to each other in solution.

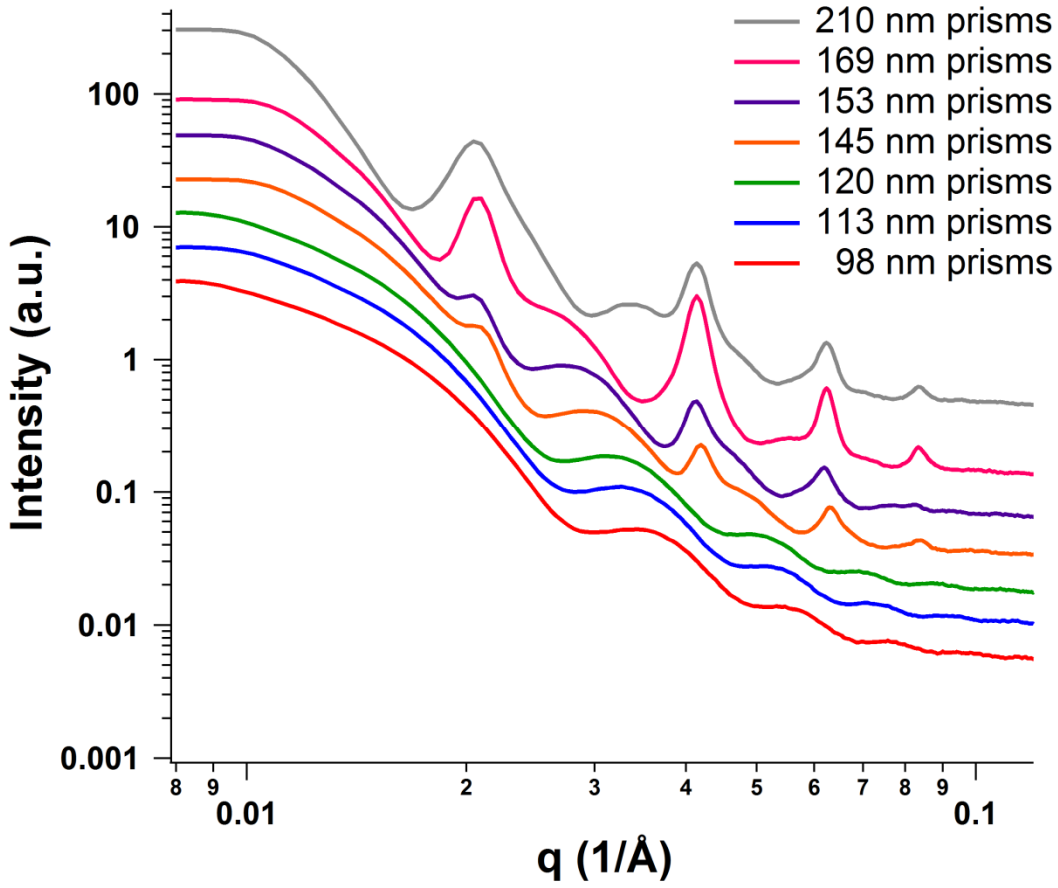

Fig. S6. One-dimensional SAXS profiles of nanoprisms with various edge lengths ranging from 98 nm to 210 nm. The SAXS profiles for prisms with edge lengths of 145 nm or greater possess 4 sharp diffraction peaks indicative of lamellar superlattices, while those with edge lengths of 120 nm or smaller do not.

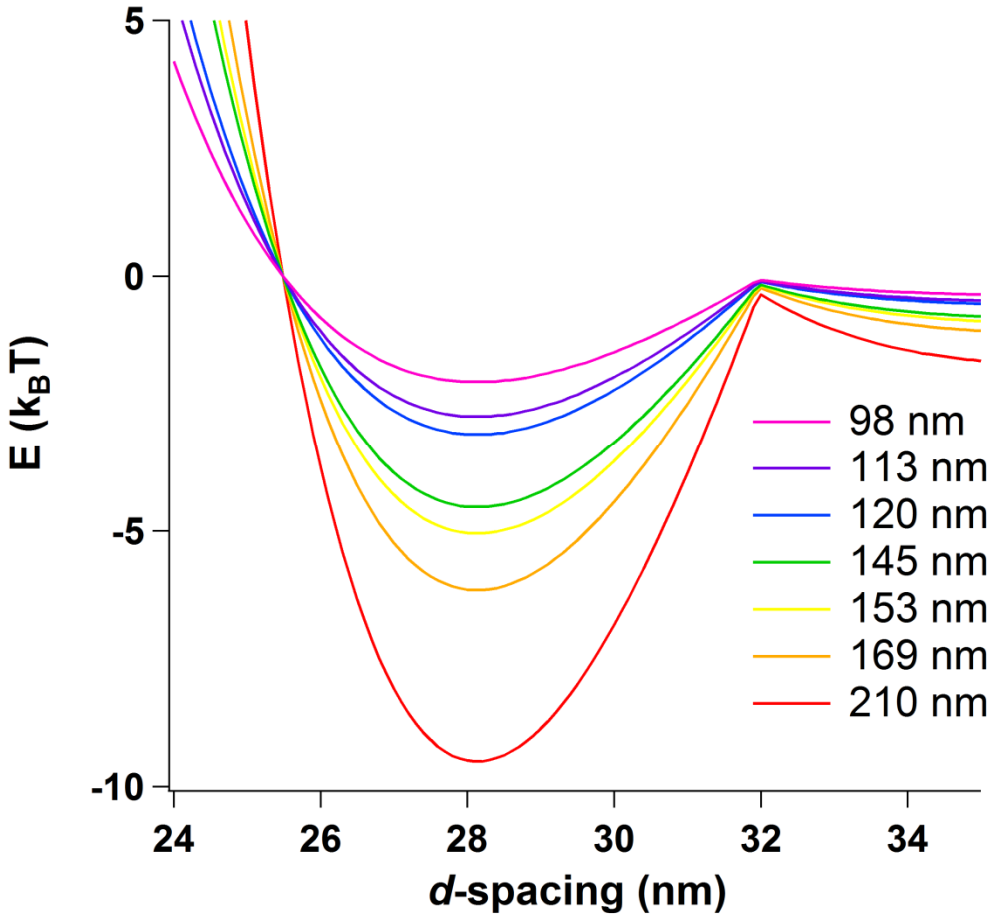

Fig. S7. The interaction free energy (in units of k_BT) between two nanoprisms of a specified edge length within a lamellar superlattice in a solution of 0.05 M CTAB taking into account van der Waals, electrostatic, and depletion interactions. The energy minimum becomes deeper as the nanoprism edge length increases.

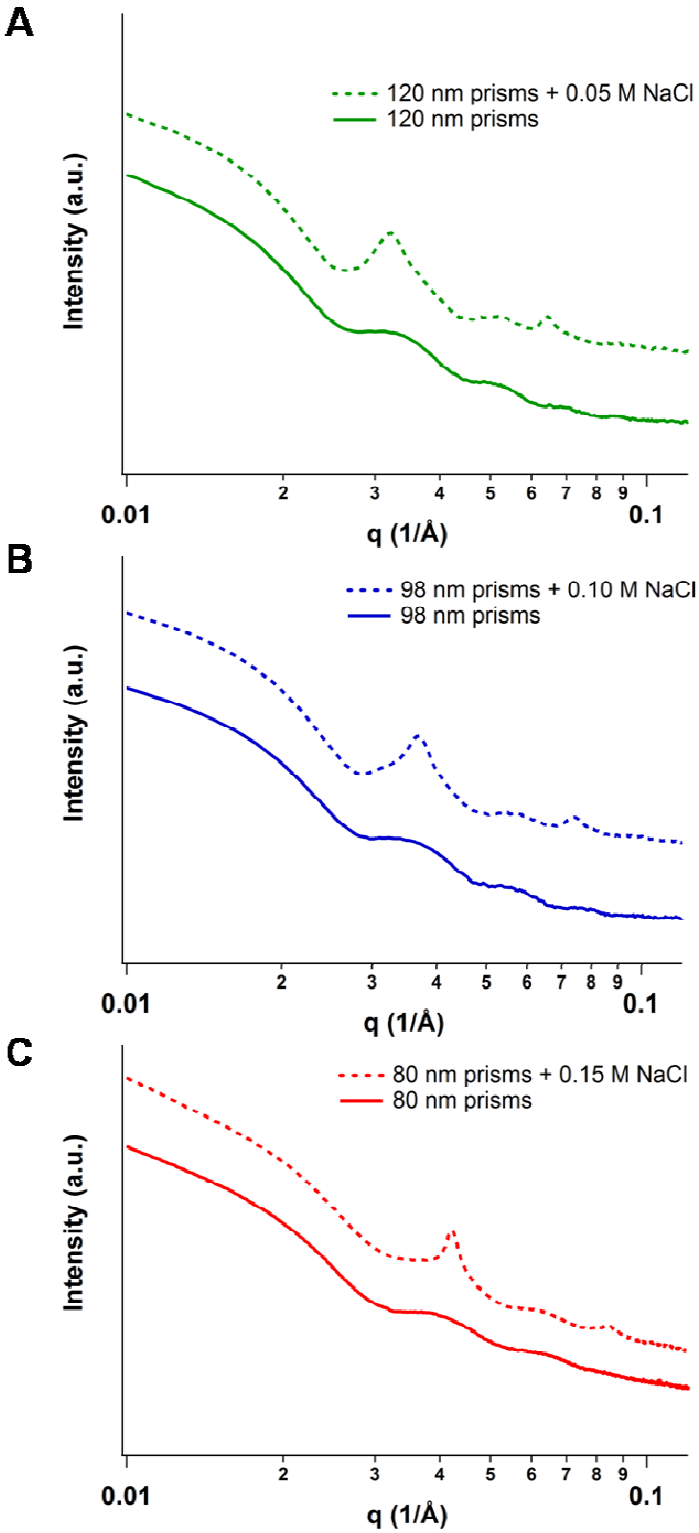

Fig. S8. One-dimensional SAXS profiles of (A) 120 nm, (B) 98 nm, and (C) 80 nm edge length nanoprisms before and after the addition of 0.05 M, 0.10 M, and 0.15 M NaCl, respectively. After the addition of NaCl, the emergence of sharp diffraction peaks indicates the presence of lamellar nanoprism superlattices in solution.

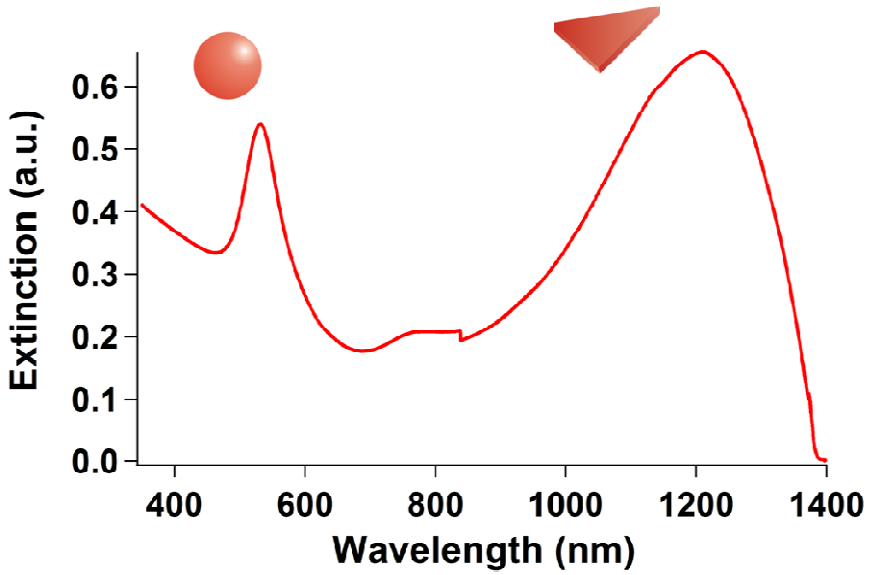

Fig. S9. UV-Vis-NIR spectrum of as-synthesized gold nanoprisms (145 nm edge length) and spherical gold nanoparticles (38 nm diameter).